Quantum Liquid with Strong Orbital Fluctuations: The Case of a Pyroxene Family

A. E. Feiguin,[1] A. M. Tsvelik,[2] Weiguo Yin,[2] and E. S. Bozin[2]
[1]Department of Physics, Northeastern University, Boston, Massachusetts 02115, USA
[2]Condensed Matter Physics and Materials Science Division, Brookhaven National Laboratory, Upton, New York 11973, USA

(Received 29 August 2019; published 3 December 2019)

We discuss quasi-one-dimensional magnetic Mott insulators from the pyroxene family where spin and orbital degrees of freedom remain tightly bound. We analyze their excitation spectrum and outline the conditions under which the orbital degrees of freedom become liberated so that the corresponding excitations become dispersive and the spectral weight shifts to energies much smaller than the exchange integral.

DOI: 10.1103/PhysRevLett.123.237204

Introduction.—During the last 30 years a great theoretical effort has been directed at the research on quantum liquids where spin ordering either does not occur or the transition temperature is strongly reduced by fluctuations. Quantum liquids play an important role in all kinds of theoretical scenarios for exotic matter states. Quantum fluctuations increase when the symmetry manifold is extended from the ubiquitous SU(2) to a higher symmetry, for instance, SU(N). In practice such extension can occur only when orbital degrees of freedom (d.o.f.) are included which is difficult since the orbital degeneracy is usually lifted by the lattice. In this Letter we suggest that magnetic insulators from the so-called pyroxene family may provide a possible path to overcome these difficulties.

Pyroxenes are quasi-one-dimensional Mott insulators where spin and orbital d.o.f. remain tightly bound even at low energies. They compose a rich class of minerals with chemical formula $AM(\mathrm{Si,Ge})_2\mathrm{O}_6$ where A is mostly an alkali metal element and M a trivalent metal element. For example, greenish $\mathrm{NaAlSi_2O_6}$ is a famous Chinese jade called Fei Tsui. The systems with partially filled d shells of the M ions commonly possess nontrivial magnetic properties ranging from antiferromagnetic (AF), ferromagnetic (FM), and spin glassy and likely to be multiferroics, as seen in $\mathrm{NaFeSi_2O_6}$, $\mathrm{LiFeSi_2O_6}$, and $\mathrm{LiCrSi_2O_6}$ [1]. Their crystal structures contain characteristic *zigzag* chains of edge-sharing $M\mathrm{O}_6$ octahedra (Fig. 1). The chains are bridged by the O-Si-O or O-Ge-O bonds, or, in other words, are separated by $\mathrm{SiO_4}$ or $\mathrm{GeO_4}$ tetrahedra, thus confining the motion of valence electrons to the chains.

In this Letter we discuss pyroxenes with $M =$ Ti and Ru, where the lowest t_{2g} orbitals well separated from the e_{2g} ones are occupied either by a single electron (Ti) or a single hole (Ru). At present only $\mathrm{NaTiSi_2O_6}$ has been experimentally studied. Like the V^{4+} ions in the straight-chain system $\mathrm{VO_2}$, the Ti^{3+} ions in $\mathrm{NaTiSi_2O_6}$ have the $3d^1$ valence electron configuration and undergo the Ti-Ti dimerization upon cooling. The zigzag chain pattern makes it more apparent that all spin, orbital, and lattice d.o.f. are active, leading to two-orbitally assisted Peierls transition [2–4] that generates spin-singlet dimers on the short Ti-Ti bonds [5] with the spin gap of ∼53 meV [6], rather than a gapless long-range antiferromagnetic (AF) state in $\mathrm{VO_2}$. Note that the ordinary spin-Peierls transition seems not to work here because the doubled periodicity is not consistent with the quarter filling of the electronic bands. An early density-functional theory (DFT) study focused on the high-temperature nondimerized structure of $\mathrm{NaTiSi_2O_6}$ attributed the spin gap to the spin-one ($S = 1$) Haldane type due to the ferromagnetic Ti-Ti interaction [7]. A subsequent DFT calculation with a U correction showed that the dominant magnetic interaction was the AF one along the Ti-Ti short bonds, supporting the picture of $S = 0$ spin dimers [8]. However, an outstanding puzzle is that the heat capacity data show the gap ∼10 meV [5] suggesting the existence of softer excitations and stronger quantum fluctuations.

We approach the problem using a combination DFT, analytic, and time-dependent density-matrix renormalization group (DMRG) methods to study their orbital and spin dynamics. The stronger quantum fluctuations originate from the involvement of the third t_{2g} orbital, which becomes active when the oxygen-atom-mediated electron hopping integral is comparable to the direct hopping integral between neighboring M atoms [1,9,10].

Hubbard model and the Sutherland Hamiltonian.—We start with a microscopic derivation of the three-orbital model Hamiltonian [11] assuming a single electron or hole occupation of the t_{2g} orbital. The strong on site Coulomb interaction $U(N-1)^2$ opens a charge gap $\sim U$ preventing direct transitions to states with different occupation number. To describe the low energy dynamics we have to integrate out the high-energy d.o.f. as it is done in the conventional SU(2) invariant Hubbard model [17]. Here, each M cation is coordinated with six O^{2-} anions and the $M\mathrm{O}_6$ octahedra are edge sharing to form the zigzag chain in

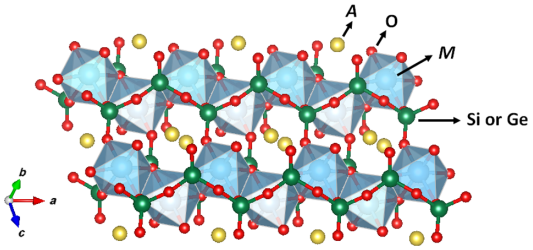

FIG. 1. Crystal structure of Na $M\mathrm{Si_2O_6}$.

the crystallographical a axis (Fig. 1). The five d-shell orbitals of the M ion are well separated by the ligand field into the high-energy e_g ($3z^2-r^2$ and x^2-y^2) and low-lying t_{2g} (xy, yz, zx) orbitals. The latter orbitals are relevant to the low-energy physics. If one neglects all factors leading to violation of the SU(6) symmetry, such as the splitting of the t_{2g} orbitals and the Hund's interaction and adopts a diagonal tunneling matrix with identical matrix elements t for all orbitals, the result for $U \gg t$ is the SU(6)-symmetric Sutherland Hamiltonian:

$$H = J\sum_k P^{o,s}_{k,k+1}, \qquad J = \frac{2t^2}{U}, \tag{1}$$

where $P^{o,s} = P^o \otimes P^s$ is the permutation operator acting in 6×6-dimensional space of spin and orbital quantum numbers and $P^s_{k,k+1} = 2\boldsymbol{S}_k\cdot\boldsymbol{S}_{k+1} + 1/2$ and $P^o_{k,k+1} = 2\boldsymbol{T}_k\boldsymbol{T}_{k+1} + 1/2$, where S^a, T^a are spin and isospin $S = 1/2$ operators acting on the spin and orbital subspaces, respectively. Model (1) is integrable, the spectrum consisting of collective orbital and spin excitations is gapless [18]. The excitations (spinons) are fractionalized, they carry spin and orbital quantum numbers of electrons (except the charge one which is gapped). The spin spectral function is presented on Fig. 2(a).

In reality the SU(6) symmetry is broken due to the crystal field and anisotropy of the exchange integrals originating from (i) the difference between tunneling matrix elements of different orbital states and (ii) the Hund's coupling. Since the lowest d orbital is occupied by one electron (hole), the Hund's coupling affects only the excited states. As shown in Fig. 3(a), the strong electron hopping integrals are the head-on $d_{zx}-d_{zx}$ (between the first and second M atoms) and the head-on $d_{xy}-d_{xy}$ (between the forth and fifth M atoms), whose strength is referred to as t_1 [depicted as solid arcs in Fig. 3(b)]. Yet, for the edge-sharing t_{2g} connections, it is known that the oxygen p-orbital-mediated shoulder-to-shoulder hopping paths, e.g., the $d_{zx}-p_z-d_{yz}$ between the second and third M atoms in Fig. 3(a), may be as strong [1,9,10]. These indirect paths are referred to as t_2 [the dashed lines in Fig. 3(b)]. Note that the M yz orbitals are involved in the t_2 paths only [Fig. 3(b)]; therefore, in the limit of small t_2 or large t_{2g} splitting Δ (i.e., the yz orbital is higher in energy by Δ than the xy and zx orbitals), d_{yz}

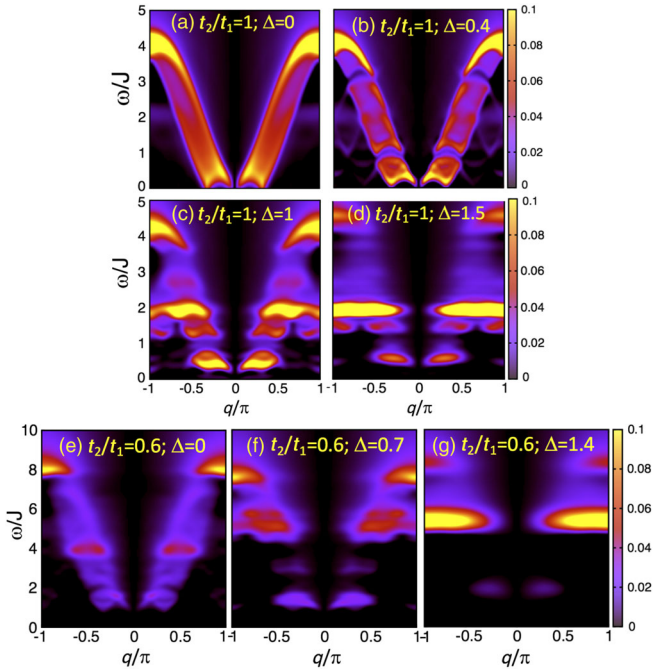

FIG. 2. Spin spectral function in the folded Brillouin Zone for various values of t_2/t_1 and the crystal field. With increase of Δ/J or the anisotropy the spectral weight shifts toward the dimerized configuration where the singlet-triplet gap is equal to $2J = 4t_2^2/(U-\Delta)$ corresponding to the breaking of a dimer.

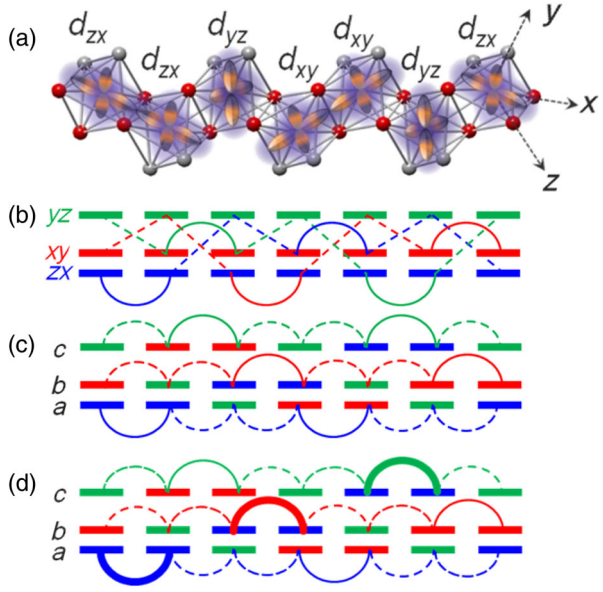

FIG. 3. (a) A graphic description of a dimerized state for an isolated Na$M\mathrm{Si_2O_6}$ chain. Only t_{2g} orbital of M ions are depicted. (b) The original tunneling scheme. (c) The tunneling scheme with relabeled orbitals. We relabel the orbitals on different sites to make the tunneling diagonal. The solid lines correspond to matrix element t_1, the dashed lines corresponds to matrix element t_2. (d) The dimerization pattern in the presence of crystal field. The orbitals on which spin singlets form are shown by thick lines.

becomes irrelevant, yielding the minimal two-orbital model [2–4]. On the other hand, for a considerable t_2 and small Δ, the t_1 and t_2 paths seem to be highly entangled as shown in Fig. 3(b); however, following the red, blue, and green lines, we found that they can be completely decoupled to form three degenerate hopping paths as shown in Fig. 3(c). In this sense, the most remarkable property of $NaMSi_2O_6$ is that its electronic band is exactly three times as degenerate. In real space the degeneracy is reflected as the following property of the single electron wave functions: $\psi_b(k+1)=\psi_b(k)=\psi_c(k-1)$.

The corresponding band Hamiltonian in notations depicted on Fig. 3(c) has three M sites in the unit cell and is expressed as follows:

$$H=-\sum_{k,\alpha=a,b,c}\psi^{+}_{\alpha,\sigma}(k)\begin{pmatrix}0 & t_1 & t_2e^{-3ik}\\ t_1 & 0 & t_2\\ t_2e^{3ik} & t_2 & \Delta\end{pmatrix}\psi_{\alpha,\sigma}(k).$$

The spectrum is determined by the cubic equation

$$\epsilon^3-\epsilon^2\Delta-\epsilon(2t_2^2+t_1^2)+\Delta t_1^2-2t_1t_2^2\cos 3k=0. \quad (2)$$

At $t_1=t_2$, $\Delta=0$ the solution is $\epsilon=2t\cos k$. The band is 1/6th filled with $k_F=\pi/6$. At $t_2\neq t_1$ and $\Delta\neq 0$, spectral gaps appear at $k=\pm\pi/3$, $\pm 2\pi/3$ corresponding to the perturbations with wave vectors $q=\pm 2\pi/3, \pm 4\pi/3$. Since they do not coincide with $2k_F$, the weakly interacting electron system would remain gapless [19]. However, for the Mott insulator this is no longer the case. Besides the charge (Mott) gap the anisotropy generates spectral gaps in all other sectors. This is obviously related to the fact that the perturbations around the SU(6) symmetric point generate relevant operators with the wave vector $4k_F$.

Integrating over the high energy states we obtain the following Hamiltonian:

$$H=\frac{2t_2^2}{U-\Delta}\sum_k P^{o,s}_{k,k+1}+\Delta\sum_k[X_{aa}(3k+2)+X_{bb}(3k)+X_{cc}(3k+1)]\hat{I}+\sum_k\delta V_k, \quad (3)$$

$$\begin{aligned}\delta V_k=&\,2\left(\frac{t_1^2}{U}-\frac{t_2^2}{U-\Delta}\right)\\ &\times[\hat{P}^s_{3k,3k+1}X_{aa}(3k)X_{aa}(3k+1)+\hat{P}^s_{3k+1,3k+2}X_{bb}(3k+1)X_{bb}(3k+2)+\hat{P}^s_{3k+2,3k+3}X_{cc}(3k+2)X_{cc}(3k+3)]\\ &+2t_2\left(\frac{t_1}{U}-\frac{t_2}{U-\Delta}\right)\{[\hat{P}^s_{3k,3k+1}X_{ab}(3k)X_{ba}(3k+1)\\ &+\hat{P}^s_{3k+1,3k+2}X_{ab}(3k+1)X_{ba}(3k+2)+\hat{P}^s_{3k+2,3k+3}X_{ac}(3k+2)X_{ca}(3k+3)]+\text{H.c.}\}+\frac{2t_2(t_1-t_2)}{U-\Delta}\\ &\times\{[\hat{P}^s_{3k,3k+1}X_{ac}(3k)X_{ca}(3k+1)+\hat{P}^s_{3k+1,3k+2}X_{bc}(3k+1)X_{cb}(3k+2)+\hat{P}^s_{3k+2,3k+3}X_{bc}(3k+2)X_{cb}(3k+3)]+\text{H.c.}\},\end{aligned} \quad (4)$$

where $P^s_{k,k+1}$ is the spin permutation operator and X_{ab} are Hubbard operators acting on orbital indices, defined as $(X_{pq})^{\alpha\beta}=\delta^\alpha_p\delta^\beta_q$. In [11] where the derivation is given, this Hamiltonian is written in terms of the isospin operators T^a. Since the Hund's coupling is just affects the anisotropy of the exchange integrals, we set it to zero to simplify the calculations restricting the consideration to various values of t_2/t_1 and Δ.

To get the overall picture of the correlations, we used the DMRG method [20,21] to calculate the imaginary part of the correlation function:

$$S(\omega,q)=\sum_k\int_0^\infty dt\langle S^z_k(t)S^z_m(0)\rangle e^{i\omega t+iq(k-m)}, \quad (5)$$

where S^z_k is the spin projection operator acting on site k. The spectral weight contains rich information about the excitation spectrum of the model. We carry out calculations with a Suzuki-Trotter decomposition of the evolution operator [22,23] and a time step $\delta t=0.1$ in units of $1/J$. We have been able to study chains with up to 48 unit cells ($L=144$ sites) using up to 1600 DMRG states for the time evolution, and 5000 for ground state calculations, that translates into a truncation error of 10^{-5} and 10^{-8}, respectively, for the gapless case (similar accuracy is obtained in the gapped case with a smaller basis size). Most time-dependent simulations were conducted on chains with 24 unit cells ($L=72$ sites). The local space of configurations has dimension of 6, but we use $U(1)$ symmetry corresponding to S^z and density conservation for each orbital channel (four quantum numbers in total). The density for each orbital sector is fixed at $n=1/3$, while the spin is set to $S^z=0$. This is equivalent to density $n=1/6$ in the $SU(6)$ chain [24]. We calculate the spectral function in real time and space with open boundary conditions, and Fourier transform it to obtain resolution

in momentum and frequency following the prescription outlined in [22,23,25].

Limit of small Δ/J, $t_2/t_1 = 1$.—Having a broader aim than a particular case of $NaTiSi_2O_6$, we deem it instructive to start with the SU(6)-invariant model. The limit $\Delta = 0$, $t_2 = t_1$ allows an analytical treatment. The thermodynamics and the excitation spectrum are extracted from Bethe ansatz. At low energies the spectral function can be analyzed by means of conformal field theory. At higher energies one can also use the $1/N$ expansion.

The spectrum of the SU(6) symmetric model is gapless and the spectral weight is centered at $q = \pm\pi/3$ which corresponds to $\pm 2k_F$. The spectral function also looks squeezed into the region

$$4J \sin(q/2) \sin|k_F - q/2| < \omega < 4J \sin(q/2) \quad (6)$$

corresponding to two-spinon emission. This agrees well with $1/N$ picture where the spin operators are represented as bilinears of weakly interacting fermions. In the presence of anisotropy spectral gaps open at $q = \pm 2k_F = \pm\pi/3$ shown in Fig. 2 meaning that the anisotropy generates a relevant operator which carries momentum $4k_F$. Such an operator exists at the SU(6) quantum critical point; it transforms according to the representation of the SU(6) group with the Young tableau consisting of a vertical column with two boxes. The scaling dimension is $d = 2(1 - 1/N) = 5/3$. The presence of such perturbation also leads to spontaneous dimerization [see Figs. 3(a), 3(d), and 5]. This order breaks a discrete (translational) symmetry, all other fluctuations are gapped and short range. Obviously, small perturbations preserve the SU(6) structure of the particle multiplets such that spin and orbital excitations are degenerate. The spectral gaps grow slowly with Δ/J as shown on Fig. 4 due the high value of the scaling dimension of the perturbing operator. The SU(6) symmetry is preserved at low energies: Fig. 4 shows that at $\Delta/J < 0.4$ a difference between the gaps for excitations with different quantum numbers is practically undetectable. At larger anisotropies the multiplets will be split.

Limit of large Δ/J.—The easiest way to understand the dimerization phenomenon is to consider the limit of large crystal field. For $J = 0$ each site has two degenerate orbitals in the ground state. For sites $3n$ it may be (a, b), for sites $3n + 1 - (a, c)$, for $3n + 2 - (b, c)$ [see Fig. 3(d)], etc. At $J \neq 0$ the degeneracy is lifted and the ground state becomes dimerized. One possible sequence of occupied orbitals is $(a, a, b, b, c, c, \ldots)$ which corresponds to a nonvanishing exchange between sites $(3n, 3n + 1)$, $(3n + 2, 3n + 3)$, etc. [see Fig. 3(d)]. The other sequence is $(b, c, c, a, a, \ldots)$ with a nonvanishing exchange between $(3n + 1, 3n + 2)$, $(3n + 3, 3n + 4)$, etc. So, in the limit of infinite Δ the ground state consists of isolated periodically arranged spin dimers. Our numerical calculations demonstrate that the dimerization persists down to smallest values

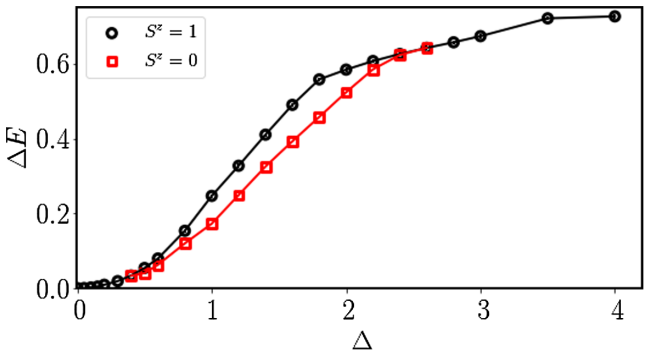

FIG. 4. Numerical results for the lowest spectral gaps for various values of the crystal field Δ and $t_2 = t_1$.

of Δ/J (see Fig. 5). It leads to two major effects for the spectrum opening gaps for all excitations and leading to a progressive shift of the spectral weight towards frequency $\omega = 2J$ corresponding to the breaking of an isolated dimer [see Figs. 2(c) and 2(d)]. Nevertheless, there is some weight at about $J/2$–13 meV, given $2J \simeq 53$ meV [6], in agreement with the gap seen in the heat capacity data [5].

According to the first-principles calculations and Wannier function analysis [11,17], $NaTiSi_2O_6$ has the following parameters: $U = 3.8$ eV, $J_H = 0.8$ eV, $t_1 = 0.203$ eV, $t_2/t_1 = 0.21$, $t_1^2/U \approx 0.01$ eV. Hence in $NaTiSi_2O_6$ the deviation from $t_2/t_1 = 1$ is quite significant. However,

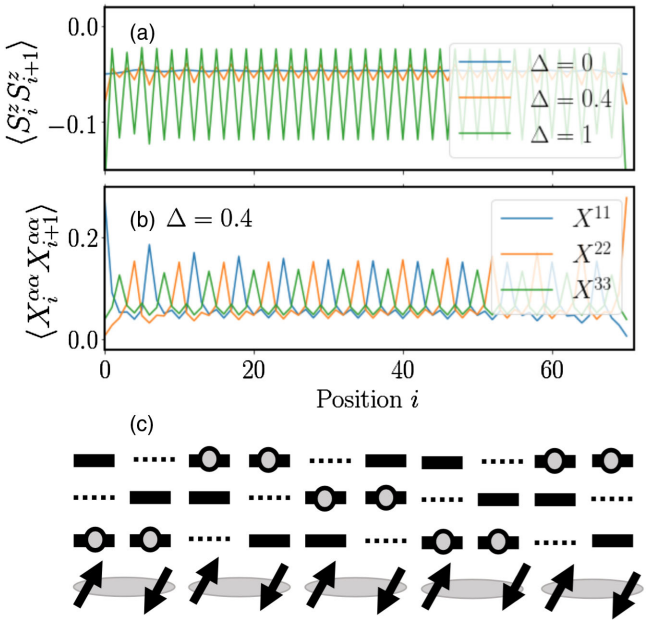

FIG. 5. Dimerization for various values of the crystal field Δ and $t_2 = t_1$. (a) Nearest neighbor spin-spin correlation; (b) density-density correlation in the orbital channel; (c) schematic illustration of the spin-orbital order in the limit of large Δ: dashed lines represent orbitals that are projected out. Charge fluctuations are suppressed and charge is frozen in the depicted pattern. Spin is only allowed to interact in pairs forming independent singlets.

due to the well-known double counting issue on the LDA + U approach to correlated materials, the value of Δ is uncertain and is taken as a free parameter. As we have seen at such values of anisotropy and crystal field the excitations are gapped and practically dispersionless [Figs. 2(d), 2(f), and 2(g)] corresponding to the local dimers discussed above. This is the situation in $NaTiSi_2O_6$ which thus fails our expectations for an orbital spin liquid. However, as follows from Figs. 2(b) and 2(c), at moderate values of the anisotropy and crystal field there is a significant spectral weight at small energies. The spectral function bears some resemblance to the SU(6)-symmetric one, which is a sign that the orbital d.o.f. are not quenched. Such situation may exist in the ruthenium- or osmium-based pyroxenes where Ru^{3+} or Os^{3+} ions contain one t_{2g} hole. These are candidates for liquids with tightly bound spin and orbital excitations. In the early $3d$ transition-metal oxides such as the titanium oxide, the $3d$ energy is considerably different from the oxygen p orbitals, which creates the barrier that hinders the indirect hopping t_2. However, t_2 may become dominant as in, for example, Na_2IrO_3 and $RuCl_3$ to induce the Kitaev-type spin frustration [10]. Specifically, considering Ru^{3+} has almost the same Shannon ionic radii as Ti^{3+}, we did similar first-principles calculations for $NaRuSi_2O_6$ [11]. We found that $t_2/t_1 = 0.64$ ($t_1 = 0.132$ eV), which is much more favorable than the $NaTiSi_2O_6$ case. In addition, the yz orbital moves higher in energy, which is closer to and mixed with the hole bands of the xy and zx characters. Moreover, the experimentally observed large bond dimerization is favored in the first-principles calculation for $NaTiSi_2O_6$, but not for $NaRuSi_2O_6$. Thus, it would be interesting to synthesize $NaRuSi_2O_6$ and compare its low-energy physical properties with the present theory.

This work was supported by the Office of Basic Energy Sciences, Material Sciences and Engineering Division, U.S. Department of Energy (DOE) under Contracts No. DE-SC0012704 (A. M. T., W. Y., and E. S. B.) and No. DE-SC0014407 (A. E. F.).

[1] S. V. Streltsov and D. I. Khomskii, Phys. Rev. B **77**, 064405 (2008).
[2] M. J. Konstantinović, J. van den Brink, Z. V. Popović, V. V. Moshchalkov, M. Isobe, and Y. Ueda, Phys. Rev. B **69**, 020409(R) (2004).
[3] J. van Wezel and J. van den Brink, Europhys. Lett. **75**, 957 (2006).
[4] T. Hikihara and Y. Motome, J. Phys. Soc. Jpn. **74** Suppl., 212 (2005).
[5] M. Isobe, E. Ninomiya, A. N. Vasili'ev, and Y. Ueda, J. Phys. Soc. Jpn. **71**, 1423 (2002).
[6] H. J. Silverstein, A. E. Smith, C. Mauws, D. L. Abernathy, H. Zhou, Z. Dun, J. vanLierop, and C. R. Wiebe, Phys. Rev. B **90**, 140402(R) (2014).
[7] Z. S. Popović, Ž. V. Šljivančanin, and F. R. Vukajlovič, Phys. Rev. Lett. **93**, 036401 (2004).
[8] S. V. Streltsov, O. A. Popova, and D. I. Khomskii, Phys. Rev. Lett. **96**, 249701 (2006).
[9] F. Mila and F.-C. Zhang, Eur. Phys. J. B **16**, 7 (2000).
[10] G. Jackeli and G. Khaliullin, Phys. Rev. Lett. **102**, 017205 (2009).
[11] See Supplemental Material at http://link.aps.org/supplemental/10.1103/PhysRevLett.123.237204, which includes Refs. [12–17], for first principles calculations and a derivation of the effective Hamiltonian.
[12] K. Schwarz, P. Blaha, and G. K. H. Madsen, Comput. Phys. Commun. **147**, 71 (2002).
[13] J. P. Perdew, K. Burke, and M. Ernzerhof, Phys. Rev. Lett. **77**, 3865 (1996).
[14] W. Ku, H. Rosner, W. E. Pickett, and R. T. Scalettar, Phys. Rev. Lett. **89**, 167204 (2002).
[15] W.-G. Yin, D. Volja, and W. Ku, Phys. Rev. Lett. **96**, 116405 (2006).
[16] R. L. Barnett, A. Polkovnikov, E. Demler, W.-G. Yin, and W. Ku, Phys. Rev. Lett. **96**, 026406 (2006).
[17] W.-G. Yin and W. Ku, Phys. Rev. B **79**, 214512 (2009).
[18] B. Sutherland, Phys. Rev. A **5**, 1372 (1972).
[19] It can be gapped by electron-phonon interaction that utilizes the $2k_F$ instability to drive the Peierls transition, in which the unit cell is doubled to have six Ti atoms, compatible with Fig. 3(d).
[20] S. R. White and A. E. Feiguin, Phys. Rev. Lett. **93**, 076401 (2004).
[21] A. Daley, C. Kollath, U. Schollwöck, and G. Vidal, J. Stat. Mech. (2004) P04005.
[22] A. E. Feiguin, in *XV Training Course in the Physics of Strongly Correlated Systems, AIP Proceedings* (American Institute of Physics, Melville, 2011), Vol. 1419, p. 5.
[23] S. Paeckel, T. Kahler, A. Swoboda, S. R. Manmana, U. Schollwöck, and C. Hubig, arXiv:1901.05824.
[24] S. R. Manmana, K. R. A. Hazzard, G. Chen, A. E. Feiguin, and A. M. Rey, Phys. Rev. A **84**, 043601 (2011).
[25] S. R. White and I. Affleck, Phys. Rev. B **77**, 134437 (2008).